CLOSED SPIRAL ANTENNA

Gheorghe MORARIU, Mihai MIRON
"Transilvania" University, Brasov, Romania
DOI: 10.19062/1842-9238.2015.13.3.10

Abstract: *The paper presents a model of fractal antenna having as resonance element a planar logarithmic spiral. The content highlights the resonance phenomenon analysis and technical design features accompanied by experimental results. Covering a very wide frequency band, having relatively small geometric dimensions and satisfactory gain, this antenna is recommended in mobile telephony, digital television and multiservice.*
Keywords: *antenna, fractal, resonance.*

1. INTRODUCTION

Fractal element antennas use fractal geometric structures as virtual combination of capacitors and coils (inductances). This allows the antenna to have several resonance frequencies that can be selected and corrected by fractal model chosen. In recent years it has been shown in many studies (Best, 2003), (Kumar, 2010), (Kumar, 2012), that the use of fractal elements in the construction of antennas provides superior properties and performances, validating the idea that geometry is a key issue in determining the unique electromagnetic behavior of antennas substantially independent of frequency (Lincy, 2013). The present paper is included in the cycle of works published by the authors and dedicated to the design and analysis of some fractal antenna types (e.g. Fractal Elliptical Segment Antenna; Fractal Sector Antenna with Resonators; Fractal Sector Stripline Antenna with Disks; Fractal Antenna with Hexagonal Resonators). Content of the work refers to a brief survey of the resonance phenomenon specific to the particular structure of the proposed antenna, the technical achievement and experimental results obtained in the process of testing the antenna.

2. THE RESONANCE PHENOMENA

Having as a resonant element the dipole formed from generated surfaces by logarithmic spirals, antenna in question is independent of radiant field polarization (admitting circular polarization) as described below.

Figure 1 shows the diagram of circular polarization on the border of a logarithmic spiral.

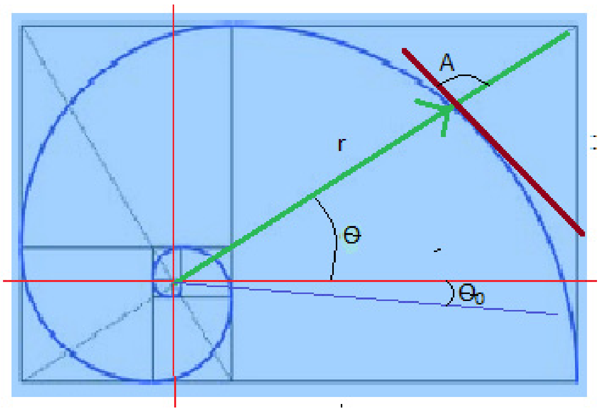

Fig. 1. The diagram of circular polarization on the border of a logarithmic spiral

$$\theta = \theta_0 + \mathrm{tg}\, A \cdot \ln r \qquad (1)$$

where: θ_0 is the angle formed by the tangent to the spiral in origin.

$$\ln r = \frac{\theta - \theta_0}{\mathrm{tg}\, A} \qquad (2)$$

$$r = e^{\frac{\theta - \theta_0}{\mathrm{tg}\, A}} \qquad (3)$$

If $r' = k \cdot r$, then

$$\theta' = \theta_0 + \mathrm{tg}\, A \cdot \ln(k \cdot r) \qquad (4)$$

$$\theta' = \theta_0 + \mathrm{tg}\, A\, (\ln k + \ln r), \qquad (5)$$

and

$$\theta' = \theta + \mathrm{tg}\, A \cdot \ln k\, . \qquad (6)$$

It results that $\mathrm{tg}\, A \cdot \ln k$ is a rotation angle.

For k=1, the spiral degenerates into a circle:

$\theta' = \theta$ and $r' = r$.

Frontier radiation

$$r = r_0 \cdot e^{\frac{\theta-\theta_0}{tg\,A}} \quad (7)$$

$$ctg\ A = b \quad (8)$$

$$r = r_0 \cdot e^{(\theta-\theta_0)\cdot b} \quad (9)$$

For $\theta_0 = 0$, the length of the spiral spring is

$$L_{sp} = \int_0^{\theta} \sqrt{r^2(\theta) - [dr(\theta)]^2}\ d\theta \quad (10)$$

$$L_{sp} = \frac{r_0}{b}\sqrt{1+b^2}(e^{b\cdot\theta} - 1) \quad (11)$$

The electric field intensity is:

$$E = \pm j \cdot Z_0 \cdot H_0 \cdot e^{j(\omega t - \varphi_0)} \quad (12)$$

Frontier radiant flux (Φ) for a segment corresponding to an opening of (0-θ) radians will be:

$$\varphi(E) = L_{sp} \cdot E \quad (13)$$

The radiant surface (S)

$$r = r_0 \cdot e^{\theta \cdot b} \quad (14)$$

$$r_0 = \rho \quad (15)$$

$$x = \rho \cdot e^{b\cdot\theta} \cos\theta \quad (16)$$

$$y = \rho \cdot e^{b\cdot\theta} \sin\theta \quad (17)$$

$$S = \int_0^{\rho}\int_0^{\theta} (y_1 - y_2)\, dx(\rho,\theta) \quad (18)$$

$$y_1 = \rho \cdot e^{b_1\cdot\theta} \sin\theta \quad (19)$$

$$y_2 = \rho \cdot e^{b_2\cdot\theta} \sin\theta \quad (20)$$

$$S = \rho^2 \left(\frac{e^{2\cdot b\cdot\theta}}{4\cdot b}\right) \Big|_0^{\rho}\Big|_0^{\theta} \quad (21)$$

$$S = \frac{\rho^2}{4}\left(\frac{e^{2\cdot b_1\cdot\theta}-1}{b_1} - \frac{e^{2\cdot b_2\cdot\theta}-1}{b_2}\right) \quad (22)$$

3. TECHNICAL ACHIEVEMENT AND EXPERIMENTAL RESULTS

The construction of the antenna is based on a divergent fractal with square surface contour and sides divided by a factor of 2, where the logarithmic spiral dipoles are cut out (figure 2) respecting the following adaptation relationships.

$$w_0 = \frac{c}{2f_0}\sqrt{\frac{2}{\varepsilon_r+1}} \quad (23)$$

$$\varepsilon_{reff} = \frac{\varepsilon_r+1}{2} + \frac{\varepsilon_r-1}{2}\left(1+12\frac{h}{w_0}\right)^{\frac{1}{2}} \quad (24)$$

$$\lambda_{c0} = 2\frac{c}{\sqrt{\varepsilon_{reff}}} \cdot \frac{1}{f_0} \cdot \frac{w_0}{L_{01}+L_{02}} \quad (25)$$

$$\lambda_{ci} = \frac{\lambda_{c0}}{2^i} \quad (26)$$

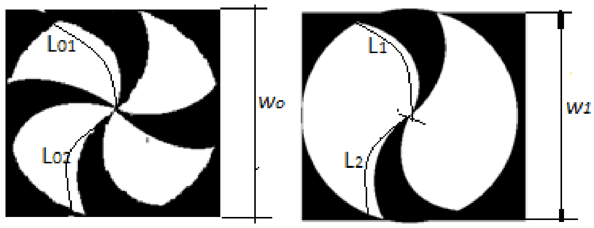

Fig. 2. The cutting of the logarithmic spiral dipoles

Take into consideration a reference frequency f_0 = 1,5Ghz and $\varepsilon_r = 2{,}25$, $\theta_1 = 34^0$, $\theta_2 = 46^0$, these values are calculated:

$w_0 = 8cm$;

$\varepsilon_{reff} = 2{,}14$;

$L_{01} = 5{,}2cm$; $L_{02} = 4{,}7cm$;

$\lambda_{c0} = 21cm$.

Corresponding to optimal wavelength λ_{ci}, i = 0 - n, for which are obtained the best antenna gain, are determined reference central frequencies of the fractal antenna.

Figure 3 and Figure 4 shows front and rear antenna architecture.

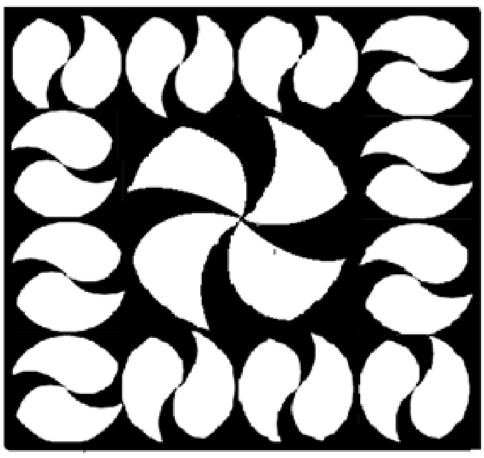

Fig. 3. The active face of the antenna

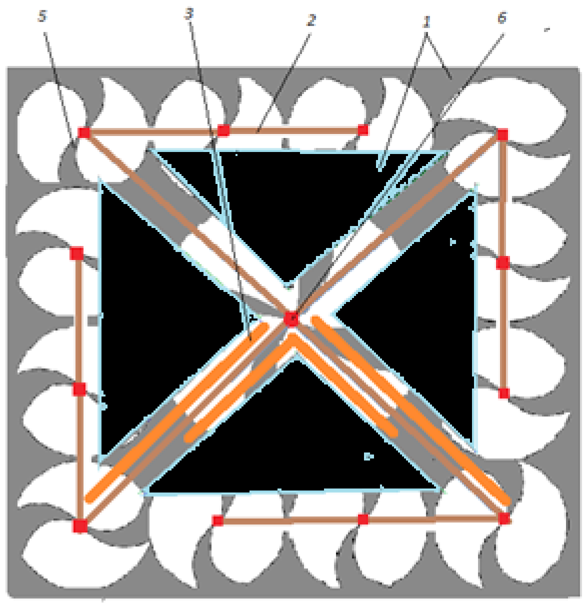

Fig. 4. Rear view of the antenna: 1- relative ground of the antenna, 2- resonator and signal collector, 3-section of line adaptation; 5- logarithmic spiral resonator; 6- signal socket

The experimental results are presented in sequential order as follows: directivity diagram, characteristic impedance variation, electric field on the central resonator, Smith charts obtained for two different frequency domains (through vector analyzer - VNA).

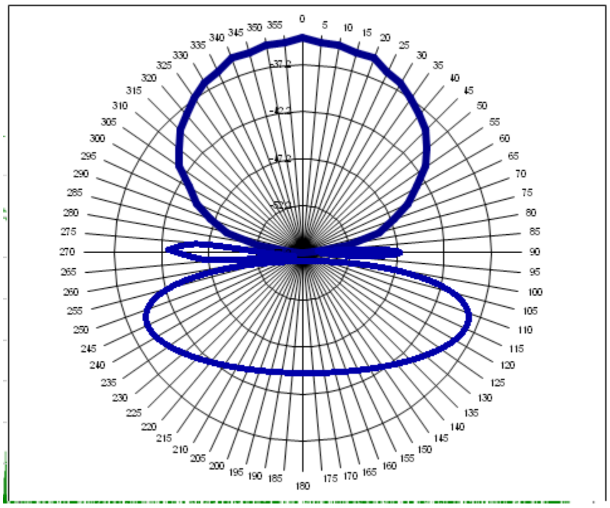

Fig. 5. Directivity diagram

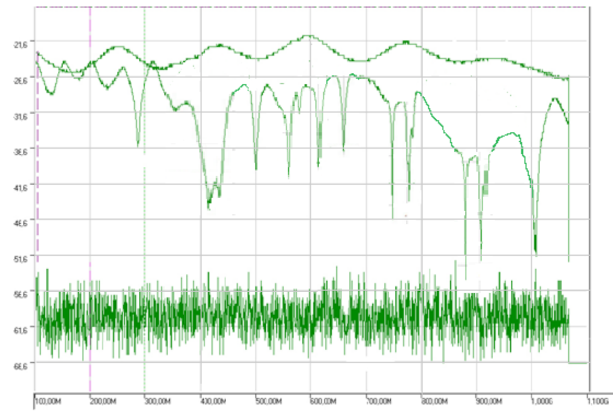

Fig. 6. VSWR for a 50Ω feeder

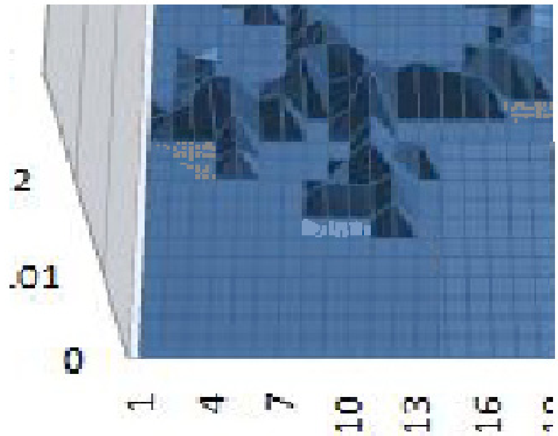

Fig. 7. Mapping of the electric field on the central resonator

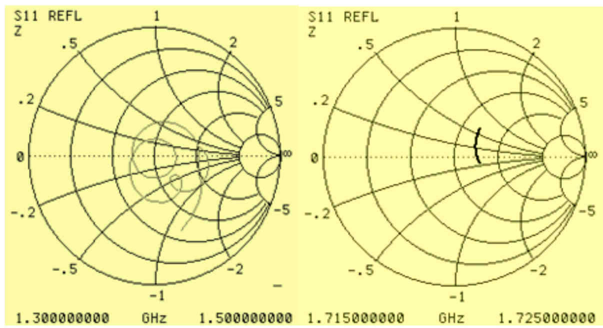

a. b.

Fig. 8. Smith charts obtained for the frequency domains: a. 1.3-1.5GHz; b. 1.715-1.725GHz

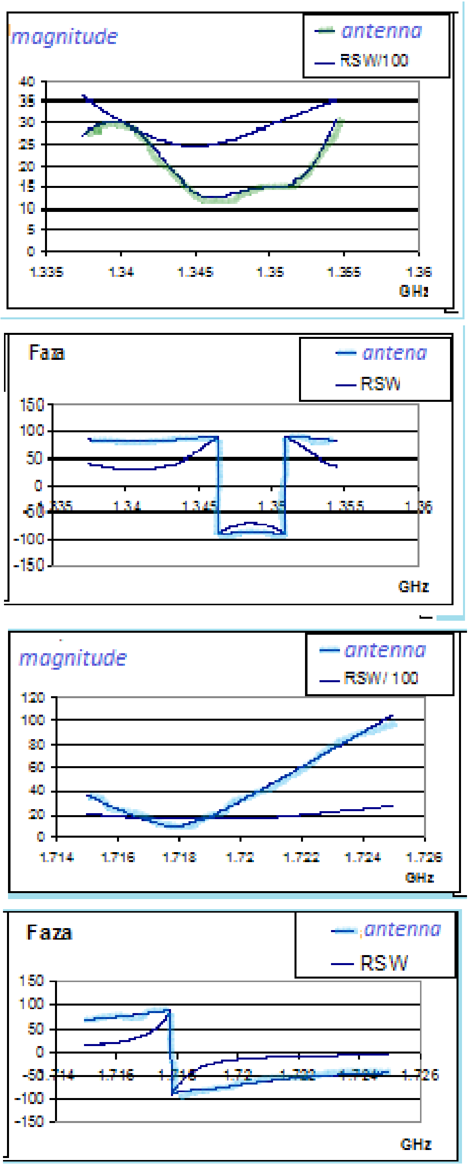

Fig. 9. VNA images for the frequency domains 1.335-1.36GHz and 1.714-1.726GHz

CONCLUSIONS

This antenna belongs to the class of fractal antennas (theoretically independent of frequency antennas) and operates in 100MHz-2.5GHz frequency band with 4-6dB gain. Through a good adaptation between fractal radiating elements and feeder it can obtain a gain of 7-8dB in a narrower frequency band.

Due to the characteristics, this antenna pattern achieved on a smaller scale can be used in digital communication; group delay can be below 2.5 periods at 2.5GHz.

BIBLIOGRAPHY

1. Best, S. (2003). *A Comparison of the Resonant Properties of Small Space-Filling Fractal Antennas.* IEEE Antennas and Wireless Propagation Letters 2 (1): 197–200.
2. Kumar, R., Malathi, P. (2010). *On the Design of CPW- Fed Ultra Wideband Triangular Wheel Shape Fractal Antenna*. IJMOT, vol. 5 no. 2, p. 89-93.
3. Kumar, R., Chaubey, P., N. (2012). *On the Design of Tree-type Ultra Wideband Fractal Antenna for DS-CDMA System*. Journal of Microwaves, Optoelectronics and Electromagnetic Applications, Vol. 11, No.1, p. 107-121.
4. Lincy, B., H., Srinivasan, A., Rajalakshmi, B. (2013). *Wideband FractalMicrostrip Antenna for Wireless Application*. ICT Journal, Volume 3 No. 3, ISSN2223-4985.
5. Morariu, Ghe., Alexandru, M., Miron, M., Romanca, M., Machedon-Pisu, M., Dobrescu, A. (2009). *Experiment-supported study on the bipolar disk microstrip antenna*. EU Annals of DAAAM & Proceedings, Vienna, Austria.
6. Morariu, G., Zara, M. (2013). *Fundamente si aplicatii ale structurilor fractale in antene pentru microunde*. Editura Universitatii Transilvania din Brasov.
7. Rop, K., V., Konditi, B., O., Ouma, H., A., Musyoki, S., M. (2012). *Parameter optimization in design of rectangular microstrippatch antenna.* IJTPE ISSN 2077-3528.